JOURNAL OF GEOPHYSICAL RESEARCH, VOL. 113, A07S02, doi:10.1029/2007JA012756, 2008

Cluster observations of the Earth's quasi-parallel bow shock

E. A. Lucek,[1] T. S. Horbury,[1] I. Dandouras,[2] and H. Rème[2]

Received 24 August 2007; revised 4 February 2008; accepted 28 February 2008; published 25 June 2008.

[1] Cluster observations of the Earth's quasi-parallel shock are used to investigate properties of the transition and the role of magnetic pulsations in the shock process. We use crossings at small spacecraft separations to show that pulsations grow in only a few seconds. We then use an example when the spacecraft were only a few thousand kilometers apart, and yet at times the shock was located within the tetrahedron formation, to demonstrate that for a period of 10 min the thickness of the shock transition was less than 2500 km and that during several shorter intervals the shock thickness was less than 1000 km. In the context of evidence for the extent of SLAMS exceeding 1000 km, this suggests that the thickness of the shock layer over which the bulk of plasma thermalization occurs can be narrow, containing one or at most a few SLAMS. The small-scale spatial properties of structures within the shock are difficult to extract independently of their time evolution, but we present a crossing at which two pairs of spacecraft observed the same magnetic signatures simultaneously. We show that signatures of these pulsations are consistent with their refraction as they are convected antisunward, as predicted by simulation work, and that they are coherent over a distance of at least 1300 km parallel to the expected shock surface.

Citation: Lucek, E. A., T. S. Horbury, I. Dandouras, and H. Rème (2008), Cluster observations of the Earth's quasi-parallel bow shock, *J. Geophys. Res.*, *113*, A07S02, doi:10.1029/2007JA012756.

1. Introduction

[2] A collisionless shock forms ahead of the Earth's magnetosphere in order to slow, deflect, and heat the supersonic solar wind plasma. The properties of the shock transition depend on the upstream plasma conditions: the solar wind velocity, which influences the strength of the shock, the plasma beta, and the angle between the interplanetary magnetic field and the normal to the shock surface (θ_{BN}) [e.g., *Tsurutani and Stone*, 1985, and references therein].

[3] When the magnetic field is nearly perpendicular to the shock normal (a quasi-perpendicular shock), and thus little magnetic flux threads the shock transition, the shock tends show a sharp transition between the upstream and downstream plasma. The processes that mediate this type of shock transition are relatively well understood [e.g., *Tsurutani and Stone*, 1985, and references therein; *Bale et al.*, 2005]. At all but the very weakest of shocks a fraction of the incoming solar wind proton population is reflected by the shock potential [e.g., *Sckopke et al.*, 1990; *Farris et al.*, 1993]. The ions gyrate in the upstream magnetic field and return to the shock surface [*Paschmann et al.*, 1982]. Having gained energy in this process, they cross the shock. The two plasma populations, transmitted and reflected ions, form an unstable population and waves are generated through plasma instabilities which in turn scatter the ions, forming a hot, thermalized downstream plasma population.

[4] When the magnetic field is nearly parallel to the shock normal any ions that are reflected do not return to the shock and can escape upstream [e.g., *Gosling et al.*, 1982]. Under these circumstances, as long as the Alfvén Mach number exceeds a value of about 4 [*Thomsen et al.*, 1993], the shock transition becomes extended in space and variable in time. Ion beam instabilities give rise to ultra-low frequency (ULF) waves which populate the foreshock region [e.g., *Le and Russell*, 1992]. Although these waves propagate sunward in the plasma frame, they are convected back toward the shock by the solar wind flow. The upstream ions can gain energy through further interaction with the ULF waves and form part of the population of energetic ions (10–300 keV) that are closely associated with the foreshock and quasi-parallel shock [e.g., *Ipavich et al.*, 1981]. Recent analysis of the suprathermal part of this population (10–30 keV) by *Kis et al.* [2004] using simultaneous two-point partial density data from Cluster showed that the suprathermal ion density decreased exponentially with increasing distance upstream of the shock and that the *e*-folding distance was found to increase approximately linearly with increasing energy, starting from about 0.5 Earth radius (1 R_E = 6378 km) for ions with an energy of 10 keV and increasing to $\sim$3 R_E for ions with an energy of $\sim$30 keV. However, although it should be noted that the Kis et al. results were obtained using data from one specific event, it is nonetheless interesting that the value of the *e*-folding distance found for the highest-energy band was about half the value obtained by *Ipavich et al.* [1981] or *Trattner et al.* [1994] from their statistical studies and that the *e*-folding

[1]Blackett Laboratory, Imperial College London, London, UK.
[2]Centre d'Etude Spatiale des Rayonnements, Toulouse, France.

0148-0227/08/2007JA012756$09.00

distance found by *Trattner et al.* [1994] for the lowest-energy band was just over 3 R_E, while the value found by *Kis et al.* [2004] was only 0.5 R_E.

[5] As the upstream ULF waves are convected antisunward, they interact with the gradient in suprathermal ion pressure, gain energy, and grow in amplitude into pulsations [*Thomsen et al.*, 1988], also termed short, large-amplitude magnetic structures (SLAMS) [*Schwartz and Burgess*, 1991]. This process has been identified observationally by *Giacalone et al.* [1993] as well as numerically by *Scholer* [1993], who found that for the growth of a wave into a pulsation to occur, the scale length of the suprathermal density gradient was required to be of the order of the wavelength of the original wave, and *Dubouloz and Scholer* [1995] who examined both the growth of pulsations from ULF waves and their subsequent evolution. Further support for the evolution of pulsations from the ULF wavefield came from simulations, which showed that the process also explained the polarization characteristics of SLAMS. ULF waves are predominantly right-hand polarized in the plasma frame, which, as they are convected antisunward over the spacecraft, leads to a left-handed sense of polarization in the spacecraft frame. In contrast pulsations are more usually right-handed in the plasma frame or of mixed polarization. However, the mechanism through which pulsations are observed to grow from ULF waves, by inhibiting the escape of hot ions upstream, also leads to the polarization reversal signature characteristic of SLAMS. SLAMS appear as enhancements in the magnetic field magnitude by a factor of at least 2, but often 3 or more, over the background magnetic field magnitude, lasting from a few to about 20 s [e.g., *Schwartz et al.*, 1992]. They are also associated with increases in the plasma number density correlated with the magnetic field enhancement and locally heated and slowed plasma [e.g., *Burgess et al.*, 2005].

[6] The role of magnetic pulsations in the shock process has also been explored both observationally and numerically, and both types of studies provide a useful framework against which to test the Cluster observations at a variety of tetrahedron scales. Early numerical simulations [e.g., *Burgess*, 1995, and references therein] showed that the high Mach number quasi-parallel shock exhibited cyclic behavior: at some times the shock transition was rather sharp while at others it became more perturbed and extended, and this concept of cyclic shock reformation helped to explain the wide variety of signatures observed by single and dual spacecraft at this type of shock. The quasi-parallel shock schematic proposed by *Schwartz and Burgess* [1991] (shown in Figure 1 of their paper) was based on dual spacecraft observations interpreted in the context of these simulation results. In their picture the shock transition is composed of an ensemble of pulsations or SLAMS. They originate in the ULF wavefield, growing and steepening as they are convected antisunward through their interaction with the energetic particle pressure gradient. Each SLAM structure turns the magnetic field, so that locally the magnetic field has an orientation akin to that at a quasi-perpendicular shock [e.g., *Mann et al.*, 1994]. The larger SLAMS start to stand in the flow [*Schwartz et al.*, 1992; *Mann et al.*, 1994] and eventually become embedded in thermalized, downstream-like plasma. Evidence of ion reflection within the quasi-parallel shock [e.g., *Gosling et al.*, 1989; *Onsager et al.*, 1990] and the more recent observation of reflected ions associated with SLAMS [*Burgess et al.*, 2005] support the concept proposed by *Schwartz and Burgess* [1991] that the patchwork of SLAMS acts to decelerate and deflect the flow and that the shock transition is thus intrinsically extended in space and reforming in time. Dual spacecraft observations [*Greenstadt et al.*, 1982] suggested that the correlation lengths within SLAMS were $\sim$1000 km, shorter than the correlation length of $\sim$1 R_E observed within ULF waves [*Le and Russell*, 1990], but without multipoint observations it was not possible to establish whether the overall size of SLAMS was smaller than that of the ULF waves. In their model *Schwartz and Burgess* [1991] thus used the observational correlation length of the ULF waves, of 0.5×1 R_E, as a baseline SLAMS scale. A recent Cluster study by *Archer et al.* [2005], however, suggested that although the correlation scale of ULF can be in the range $1-3$ R_E in a direction parallel to the wave vector consistent with previous estimates, the correlation length in the direction perpendicular to the wave vector is in the range 8 to 18 R_E.

[7] The second useful framework against which Cluster observations can be compared is provided by simulations of the quasi-parallel shock. There have been many numerical simulations studies [e.g., *Scholer*, 1993; *Giacalone et al.*, 1994; *Scholer et al.*, 2003; *Tsubouchi and Lembège*, 2004] to study the evolution of SLAMS from the upstream wavefield and their role in the shock, but the one we concentrate on here was published by *Dubouloz and Scholer* [1995] and makes a prediction for the spatial shape and scale of the SLAMS. They used a 2-D hybrid model to simulate the region upstream of the shock. In this simulation the overall thickness of the shock, including the region where the SLAMS grew in amplitude, was of the order of $2-3$ R_E, and the overall size of the SLAMS was $\sim$1000 km parallel to the bow shock normal and $\sim$3000 km in the perpendicular direction. In addition they showed that as the SLAMS were convected antisunward, approaching the nominal shock location, they became refracted, e.g., as shown in Figure 4 in their paper. By this process the SLAMS moved from sharing the alignment of the ULF waves from which they grew, to being aligned with the orientation of the expected shock surface: a definite prediction to test using observational data.

[8] In this paper we use Cluster multipoint data to address some open questions including the spatial extent of the quasi-parallel shock, the overall size and shape of the magnetic pulsations, and the variation of these properties in time and space. We use magnetic field data from FGM [*Balogh et al.*, 2001] and plasma parameters from CIS [*Rème et al.*, 2001] at a range of Cluster tetrahedron scales. The Cluster formation has been changed once or twice a year throughout the mission. Therefore observations at different tetrahedron scales, which are sensitive to different shock processes, are made at a number of shocks with a range of plasma parameters, often during different years. This makes it difficult to combine results from different tetrahedron scales. The situation is further complicated by the relatively low incidence of well-developed quasi-parallel shocks in the Cluster data set. Therefore we have not yet been able to make a comprehensive multispacecraft survey of quasi-parallel

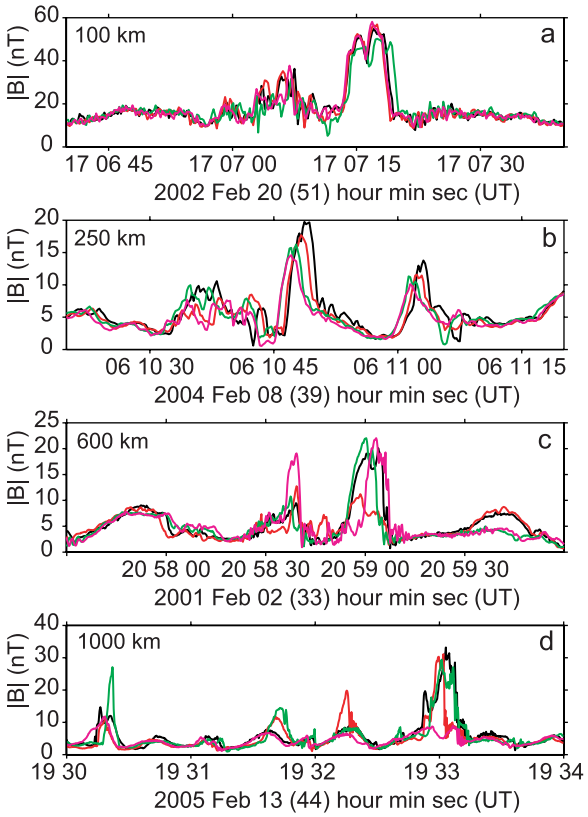

Figure 1. (a to d) Four examples of SLAMS within quasi-parallel shock transitions (note that the timescales vary between examples), with the magnetic field magnitude in nT (|B|) shown from each of the four spacecraft (Cluster 1: black. Cluster 2: red. Cluster 3: green and Cluster 4: magenta). The approximate tetrahedron scale in kilometers is given.

shock properties under a range of plasma conditions. Instead we use a combination of case studies and statistical analysis to study the shock for comparison with results from previous work.

[9] Previous single and dual spacecraft observations of SLAMS were not able to determine their overall size or shape or how rapidly they grow. Cluster multipoint data can be used to place some constraints on the size and shape of SLAMS. Therefore, in this paper, we start by presenting examples of how SLAMS appear at the four spacecraft for a series of different spacecraft separation distances. This is followed by a statistical analysis of SLAMS observed at different pairs of spacecraft in order to identify a signature of time evolution. Numerical simulations show evidence for the rapid growth of pulsations on the order of a few seconds, but with Cluster observations over a range of spacecraft separations we are able to test on what timescales a signature of growth is observed. Knowledge of the maximum time over which SLAMS growth can be neglected is also important for trying to disentangle signatures of spatial variation from those arising from SLAMS growth. Observational studies before Cluster were not able to establish whether the region over which the shock transition occurred was deep, involving many SLAMS, or narrow, perhaps only involving a few, or whether both types of transition occurred within a shock reformation cycle. We present a case study here that allows us to place an upper limit on the overall shock thickness for a particular example. Finally, we address the evolution of SLAMS properties as they are convected toward the shock. We know from previous observations that SLAMS grow in amplitude and sunward velocity, but no evolution in orientation had been identified. We use two approaches to address this question: first, we analyze a sample of SLAMS observed by Cluster at small separation scales, and finally, we use a second case study to present evidence for the refraction of SLAMS as they approach the shock, as predicted by *Dubouloz and Scholer* [1995].

2. Cluster Observations of the Earth's Quasi-Parallel Bow Shock

2.1. Four Spacecraft SLAMS Observations and Different Tetrahedron Scales

[10] The difference in appearance of SLAMS at the four Cluster spacecraft depends strongly on the tetrahedron scale. Figure 1 shows examples of SLAMS measured by all four spacecraft, at four different spacecraft separations. In Figures 1a–1d the magnetic field magnitude in nT is plotted from each of the four spacecraft (note that the subplots do not all use the same timescale). Figures 1a to 1d show examples of SLAMS at increasing tetrahedron separations: 100, 250, 600, and 1000 km. For context, 100 km is of the order of the ion inertial length, while the gyroradii of hot ions, with energies greater than the thermal solar wind beam, (~1.4–30 keV) is of the order of 1000–3000 km.

[11] At the smallest tetrahedron separation of 100 km (Figure 1a), the four spacecraft typically observe a very similar SLAMS profile with time delays between the spacecraft of a second or less. On these timescales there is no evidence for time evolution of the SLAMS (as discussed in section 2.2), and thus we interpret small differences in SLAMS profile between spacecraft as arising from spatial gradients in the SLAMS magnetic field structure. Interpretation of the data in this way suggests that the minimum spacecraft separation at which spatial variations become statistically significant is of the order of 100–150 km [*Lucek et al.*, 2004, *Lucek*, 2006].

[12] When the tetrahedron scale is approximately 250 km (Figure 1b), the SLAMS frequently, though not always, have a signature that is consistent with their growth as they cross the four spacecraft. At this scale the time delays between pairs of spacecraft are of the order of a few seconds. As shown in the next section, although spatial gradients in the magnetic field do contribute to the inter-spacecraft differences at this scale [*Lucek et al.*, 2004], there is also a statistically significant signature of SLAMS growth.

[13] Figure 1c shows an interval containing two SLAMS, observed when the spacecraft tetrahedron was of the order of 600 km, and Figure 1d shows a sequence of SLAMS observed when the spacecraft were around 1000 km apart. In both of these cases, a SLAM structure is generally observed by all four spacecraft, but there are significant differences between them, both in overall SLAMS amplitude and in the details of the profile. We expect a contribu-

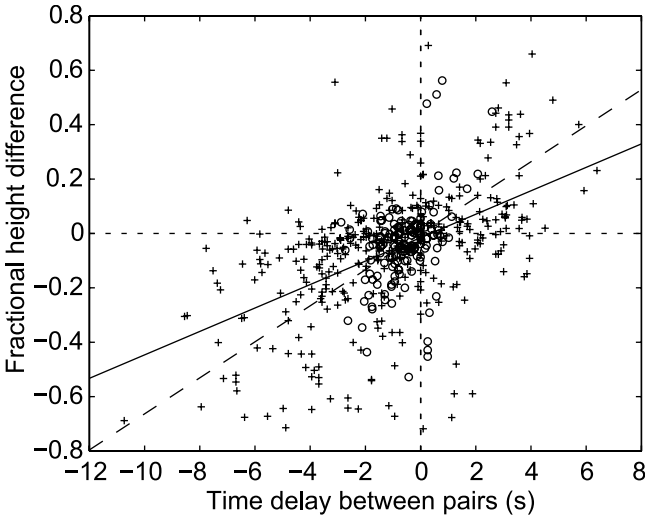

Figure 2. Scatterplot showing the change in size of a SLAM structure observed by two spacecraft as a function of the time delay in the observation times. The difference in SLAMS size is normalized by the maximum SLAMS size observed by any of the four spacecraft. Crosses show data from 2005 and the straight line fit is plotted in a solid line. Open circles show data from 2004, and the best fit straight line is shown using a dashed line.

tion to these differences from time evolution. In addition some differences are likely to arise from occasions when one or more of the spacecraft pass through the edge of the structure. However, the level of the differences between profiles, even when the magnitudes are similar, is greater than that generally seen for ULF wave profiles measured by Cluster at the same tetrahedron scale. This result, visible in the earliest Cluster data [*Lucek et al.*, 2002] was surprising because it suggested that although the overall size of SLAMS exceeded 600 km, there was in addition significant spatial variation on these scales. However, using the small sample of SLAMS available at that time, it was not possible to establish the relative contributions to the interspacecraft differences of time evolution and spatial variation. In section 2.4 we will present a case study suggesting that in at least one case, SLAMS can be coherent over several thousand kilometers. Figure 1d shows a sequence of ULF waves with a period of about 30 s, visible as small enhancements in |B|, and SLAMS which reach significantly larger values of |B|. This interval suggests that both spatial variation and time evolution have significant effects on the signatures seen at tetrahedron scales of 1000 km. There are four SLAMS, the first just after 1930 UT, then a sequence of three starting just after 1931:30 and the final one centered on 1933 UT. The example just after 1931:30 UT shows the most unambiguous signature of time evolution: the SLAM grows between crossing Cluster 1 and 4 and then Cluster 2 and 3 about 5 s later. However, the next example in the sequence has the largest magnitude at Cluster 2, which was the first spacecraft to encounter it, suggestive of a spatial variation in SLAMS properties.

[14] In the next three sections we use a combination of statistical analysis and case studies to explore the properties of the quasi-parallel shock transition. In order to build a more complete picture, further cases over a range of shock Mach number and plasma beta conditions are required, but these examples provide parts of a framework against which to compare future observations.

2.2. SLAMS Growth

[15] As described above, differences in SLAMS profiles between spacecraft arise, in general, from a combination of spatial variation in the magnetic field and time evolution (growth) of the SLAM structure. However, for time differences between SLAMS observations at two different spacecraft that are small relative to time over which SLAMS grow, it would be expected that any variations in the SLAMS profile between spacecraft would be dominated by spatial variations. In order to determine the time delay over which a statistically significant signature of SLAMS growth could be seen, the fractional change in SLAMS size between pairs of spacecraft was plotted as a function of the delay between the first and second spacecraft observation times, as shown in Figure 2. Here the fractional change in SLAMS size was defined to be the change in height between SLAMS profiles at two spacecraft divided by the maximum height within all four spacecraft. A least squares straight line was then fitted to the data as a first-order measure of whether the data contained a signature of growth. If the differences were dominated by spatial variations only, a scatterplot with no statistically significant positive gradient would be observed. This was the case for SLAMS observed in 2002 at a tetrahedron scale of approximately 100 km, when the time differences were typically less than a second. Figure 2 shows data for SLAMS observed in 2004 (tetrahedron scale ~250 km) in circles, and the data for 2005 (tetrahedron scale ~1000 km) in crosses. The data set from 2004 includes 26 SLAMS observed during five shock crossings, and the data from 2005 includes 62 SLAMS in 23 crossings. A separate fit was made to the data from each of the 2 years. In 2004 a gradient of 0.07 ± 0.01 s^{-1} was found (dashed line): five standard errors from a zero gradient. For the larger data set from 2005 a gradient of 0.043 ± 0.004 s^{-1} was found (solid line). The gradient is smaller in the latter case, but it has a more statistically significant difference from zero of 11 standard errors.

[16] We do not interpret the fits in Figure 2 as absolute measures of the growth rate since neither would we expect SLAMS to exhibit steady growth with a linear time dependence, nor in this analysis have we attempted to identify and exclude those SLAMS which are not growing, but it is clear that if the delay between two spacecraft encountering a SLAM structure is more than a second or so, the SLAMS cannot be assumed to be static over this time. This complicates analysis of SLAMS at larger separations. These results are consistent with the estimates of SLAMS growth timescales derived from simulation work, which suggest that SLAMS growth occurs on a timescale given by the inverse of the ion gyrofrequency, giving a value of the order of a few seconds for typical solar wind magnetic field values [e.g., *Scholer et al.*, 2003; *Tsubouchi and Lembège*, 2004].

[17] Different gradients are obtained for the 2 years, taking into account the uncertainty in each estimate. This might arise from difference in the two samples of shocks if

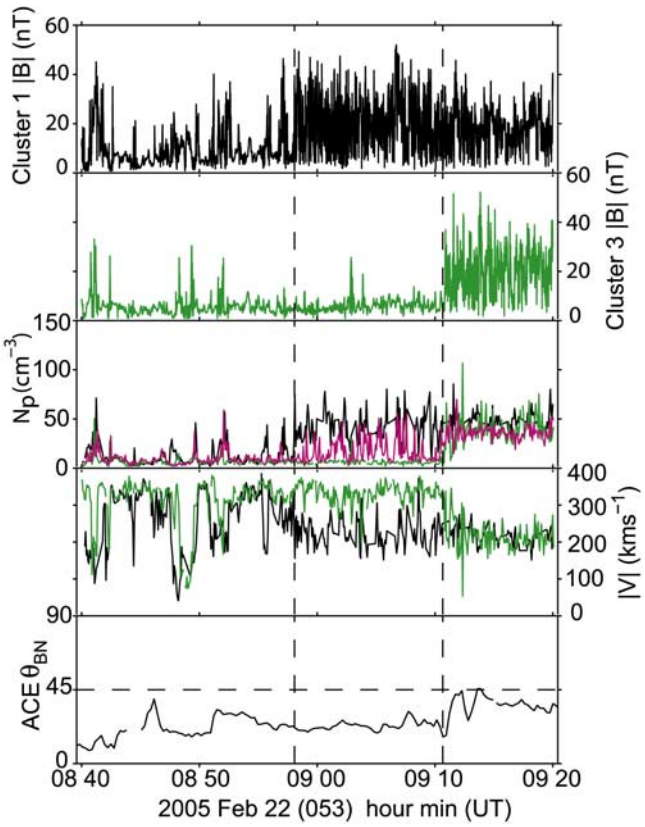

Figure 3. Data from a quasi-parallel shock crossing on 22 February 2005 (day 53). The first and second panels show magnetic field magnitude (|B|) in nT from Cluster 1 and Cluster 3, which had a separation of about 3000 km at the time. The third and fourth panels show the proton number density (N_p) in cm^{-3} and plasma flow speed (|V|) in kms^{-1} from Cluster 1 (black) and Cluster 3 (green) and, for density only, Cluster 4 (magenta). The bottom panel shows the θ_{BN} angles for the shock estimated from ACE data. The vertical dashed lines indicate the times between which Cluster 3 remained upstream of the shock while Cluster 1 was downstream in the magnetosheath.

there is a dependence of SLAMS growth rate on background plasma or shock conditions. However, since the two data sets are for two tetrahedron scales, 250 km and 1000 km, the difference in gradient might also reflect different relative contributions of spatial and temporal variations.

[18] In an ideal case we would precondition the data in order to separate, to some extent, the effects of spatial variation and time evolution. One method for this would be to select observations when the spacecraft have a small separation perpendicular to the solar wind flow vector ($R_{V\perp}$) for use in exploring SLAMS time evolution, and selecting events when the spacecraft have a small separation along the solar wind flow vector ($R_{V||}$) to explore spatial variation. However, plotting the distribution of $R_{V\perp}$ as a function of $R_{V||}$ shows that they are strongly correlated, and we are not able to divide the data set into two statistically independent subsets using these parameters.

2.3. Thickness of the Shock Transition

[19] Figure 3 shows a quasi-parallel shock crossing from 22 February 2005. This is an interesting example because the shock transition was observed to be located within the tetrahedron for over 10 min. The first and second panels show the magnetic field magnitude (|B|) in nT from Cluster 1 and Cluster 3. The third and fourth panels show the proton number density (N_p) in cm^{-3} and plasma flow speed (|V|) in km s^{-1}, respectively. On each panel data from Cluster 1 are plotted in black, and data from Cluster 3 are plotted in green. Whether a spacecraft is located upstream or downstream of the shock is most clearly seen from the ion density. Therefore in the third panel we have also plotted the density data from Cluster 4 (magenta line). The fourth panel shows the predicted θ_{BN} angle of the shock (solid black line), which remains under 45° in a quasi-parallel orientation until just after 0910 UT, when it rises to approximately 45° and Cluster 3 crosses the shock into the magnetosheath. Here θ_{BN} was calculated using a bow shock normal direction estimated using the Peredo bow shock model [*Peredo et al.*, 1995], with simplified input coefficients as described by *Horbury et al.* [2002], and magnetic field data from ACE, with an appropriate time lag from the location of ACE to that of the bow shock. The Alfvén Mach number for this shock was of the order of 6: not very unusual for the Earth's bow shock. The ion beta, however, was ~5. It is found that most of the Cluster quasi-parallel bow shocks with clear signatures of SLAMS have an ion beta in the range 1–5, a range that is also consistent with the example presented by *Schwartz et al.* [1992] and *Mann et al.* [1994].

[20] At this time Cluster was located at approximately [+7.7, −2.9, −10.5] R_E (GSE). Cluster 3 was furthest upstream, and Cluster 1 was located closest to the Earth. The tetrahedron was elongated in the X_{GSE} direction with an overall extent of about 3000 km and flattened in Y_{GSE} and Z_{GSE}, with largest interspacecraft separation in these two directions of ~500 km and ~1000 km, respectively. Cluster 2 and Cluster 4 were situated between Cluster 1 and Cluster 3 in the X_{GSE} direction. All spacecraft made several encounters with shocked and partially shocked plasma between the start of the interval at 0840 and about 0858 UT, and each spacecraft also observed multiple SLAMS during this time. However, at approximately 0858 UT Cluster 1 entered the region downstream of the shock, seen clearly in Figure 3 by the increase in proton number density and the decrease in plasma velocity, while Cluster 3 remained in the upstream region until ~0910 UT at which time it also entered the magnetosheath. The ACE estimate of θ_{BN} remained below 45° during this time. Therefore, between 0858 and 0910 the quasi-parallel shock transition lay between Cluster 1 and Cluster 3. During this time these two spacecraft were separated by only 2700 km parallel to the model bow shock normal N_{BS} and by 1200 km within the nominal shock plane. This places an upper limit on the overall thickness of the shock transition of 2700 km. Cluster 2 and Cluster 4 also made a number of shock encounters, consistent with their position between Cluster 1 and Cluster 3. Ion data are not available for Cluster 2, but Cluster 4 spent short periods, of a few minutes at a time, upstream of the shock, while Cluster 1 remained downstream (see Figure 3, third panel). This

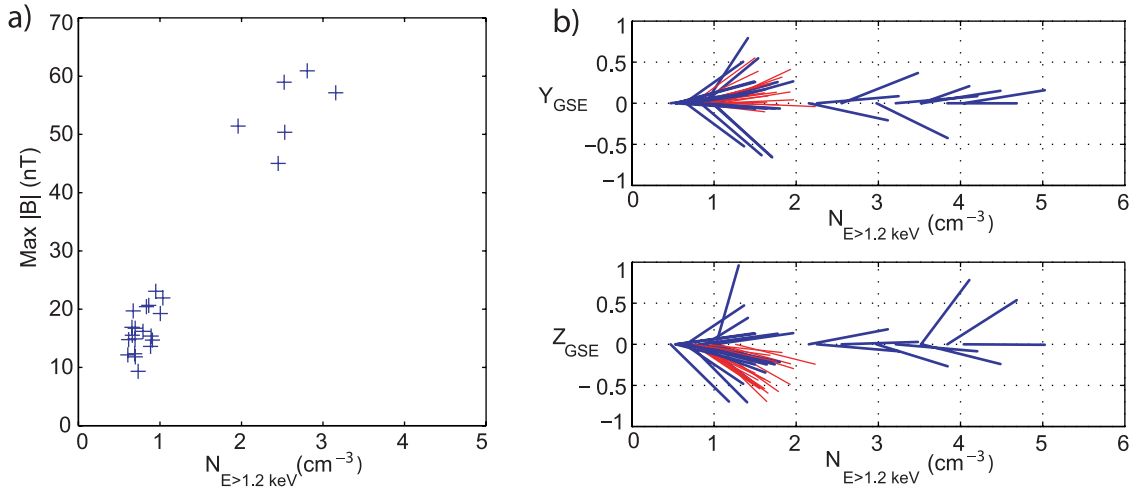

Figure 4. Properties of 28 SLAMS, observed on 2 February 2002, plotted as a function of the local number density of ions N with energies exceeding 1.2 keV ($N_{E > 1.2\ keV}$), where the lower-energy threshold is chosen to be just above the energy of the solar wind population. (a) SLAMS maximum magnetic field magnitude (|B|) plotted as a function of N. A clear dependence is seen, where larger-amplitude SLAMS tend to occur under conditions of higher N. (b) SLAMS normal directions (blue), and ULF wave normal directions (red) calculated from spacecraft timing. (top) Normals plotted as a function of X-Y $_{GSE}$, and (bottom) normals plotted as a function of X-Z $_{GSE}$, both separated in X as a function of N. The normal directions are scattered with no underlying evolution as a function of N.

further constrains the shock thickness to a maximum of just over 1000 km at these times. The multiple shock crossings made by Cluster 4 could arise from large scale shock motion, but it could also be explained by a variation in the shock thickness, perhaps as a result of shock reformation [e.g., *Burgess*, 1989].

[21] Since Figure 1 suggests that the overall size of the SLAMS is of the order of a few thousand kilometers, this in turn suggests that the quasi-parallel bow shock transition consists of at the most a few, and possibly at some times only one SLAM structure. Therefore, as simulation results suggest that SLAMS refraction occurs as a result of their slowing and deflecting the plasma, if SLAMS are indeed refracted as they approach the shock, the region in which this effect occurs might only be very close to the shock rather than a gradual effect distributed throughout the extended foreshock.

2.4. Evidence for SLAMS Refraction

[22] As described in section 2.2, the rapid growth of SLAMS complicates their analysis, including estimation of their orientation. However, it is of interest to consider whether SLAMS show a large-scale ordering and whether this changes to become aligned parallel to the expected shock surface as they are convected toward the shock as a result of refraction, as suggested by the simulations by *Dubouloz and Scholer* [1995]. In order to reduce the effect of time evolution on the results, it is necessary to consider SLAMS where the time delays between spacecraft observations are short, ideally of a few seconds or fewer. One possible way to do this is to use observations of SLAMS made with a tetrahedron scale of only ~100 km, when the time delay between SLAMS at different spacecraft is only a second or so, and on which timescale no statistically significant signature consistent with SLAMS growth is found.

[23] A sample of 28 SLAMS recorded on 2 February 2002 (day 34) was analyzed and the time delays between SLAMS observations at the four spacecraft were used to calculate an orientation and speed along the normal for each structure in the spacecraft reference frame. The results shown here were calculated following the method described by *Schwartz* [1998], which assumes that the structure can be approximated as a plane on the scale of the tetrahedron. The time delays were calculated using a cross correlation analysis between the signatures at the different spacecraft, but similar results are also obtained using the time delays between the entry (or exit) edge of the SLAMS at each spacecraft. For comparison a set of ULF waves observed a little earlier on the same day was analyzed in the same way. In order to look for a systematic change in SLAMS orientation, a measure of their distance from the shock is needed. It is known that the number density of suprathermal ions decreases with increasing distance ahead of the shock [e.g., *Kis et al.*, 2004] and so the partial density N of ions with energies E > 1.2 keV was used as a first-order measure of the location of the SLAMS relative to the shock. This method for ordering SLAMS properties was tested on SLAMS size (shown in Figure 4a) and SLAMS velocity (not shown). Both properties were well ordered by N (E > 1.2 keV): the SLAMS size increased with increasing N (E > 1.2 keV) and velocity decreased, as expected from previous observational studies [e.g., *Mann et al.*, 1994]. Figure 4a shows that the SLAMS sizes were broadly divided into two groups by plotting as a function of N. The absence of intermediate size SLAMS might reflect their rapid growth rate, but this does not explain the gap in cases with intermediate values of N (E > 1.2 keV). Despite the success of N (E > 1.2 keV) in ordering SLAMS size and velocity,

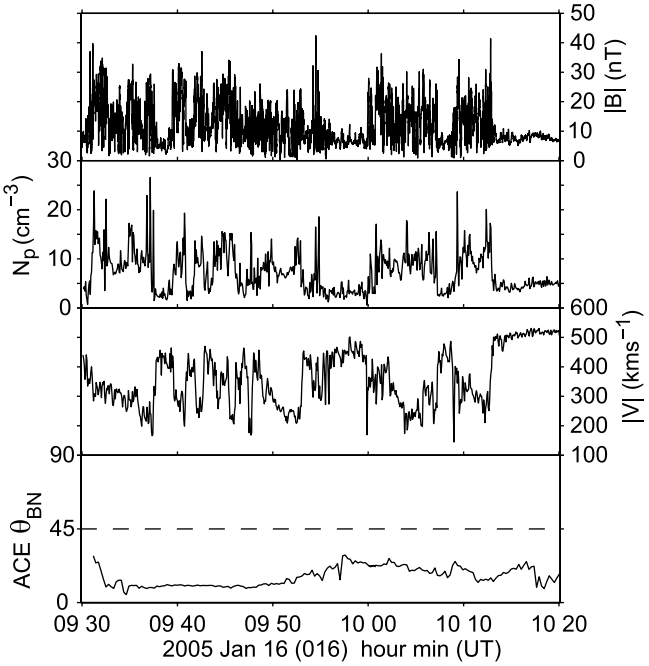

Figure 5. Data from the quasi-parallel shock crossing on 16 January 2005. Shown are magnetic field magnitude (|B|) in nT, proton number density (N_p) in cm^{-3}, and plasma flow speed (|V|) in km s^{-1}, all from Cluster 1. The bottom panel shows the θ_{BN} angle for the shock estimated from ACE data.

however, no such ordering was found for the SLAMS orientation. Figure 4b shows SLAMS normals (heavy blue lines) and ULF wave normals (faint red lines) both as a function of N (E > 1.2 keV). The ULF wave normals show quite a large variation in orientation with an average direction close to the underlying magnetic field direction (not shown). The normals calculated for the SLAMS show a larger degree of scatter, with no systematic dependence on the suprathermal number density. Neither do these normals show a systematic ordering with time, nor a dependence on the local plasma flow velocity. The range of SLAMS orientations could indicate two possibilities. First, that SLAMS do not have any underlying ordering in their orientation. The second possibility is that although the SLAMS do have a large-scale orientation, they are rippled on spatial scales of 100 km or so, and that this method of calculating a normal from the four-spacecraft timing data is sensitive to the local SLAMS orientation.

[24] In order to probe the SLAMS orientation on larger scales, observations at larger tetrahedron sizes are needed but without increasing the influence of growth on the SLAMS signatures. One opportunity that allows us to do this is when the spacecraft formation is oriented such that one or more pairs of spacecraft are separated in a direction parallel to the surface of the SLAMS. Under these circumstances the two spacecraft observe the SLAMS at nearly the same time, despite having a relatively large separation, and thus the effect of time evolution of the SLAM structure is reduced or nearly eliminated. Since a fortuitous spacecraft formation is required, analysis of this type of crossing is currently limited to a single shock case study.

[25] Figure 5 shows an overview of a quasi-parallel shock encountered on 16 January 2005 when the Cluster tetrahedron scale was of the order of a 1000 km. The first, second, and third panels show data from Cluster 1: magnetic field magnitude |B| (nT), proton number density N_p (cm^{-3}) and plasma flow speed |V| (km s^{-1}). The fourth panel shows the estimated model θ_{BN} calculated using ACE data, matched to the location of Cluster using an appropriate time delay. The estimate of the shock θ_{BN} made using ACE data indicates that the shock had a quasi-parallel orientation throughout the interval. The first through third panels show multiple transitions between shocked, partially shocked, and unshocked plasma, with a disturbed magnetic field signature characteristic of quasi-parallel shocks.

[26] In section 2.2 we showed that in at least one case of a quasi-parallel shock the shock transition was relatively narrow, less than 2700 km and at times less than 1000 km. Consequently, in our search for evidence for SLAMS refraction at the shock we concentrated on regions where the plasma velocity was changing: i.e., where the shock processes were active. Figure 6 shows such a region. In this figure the top six panels show comparisons between the

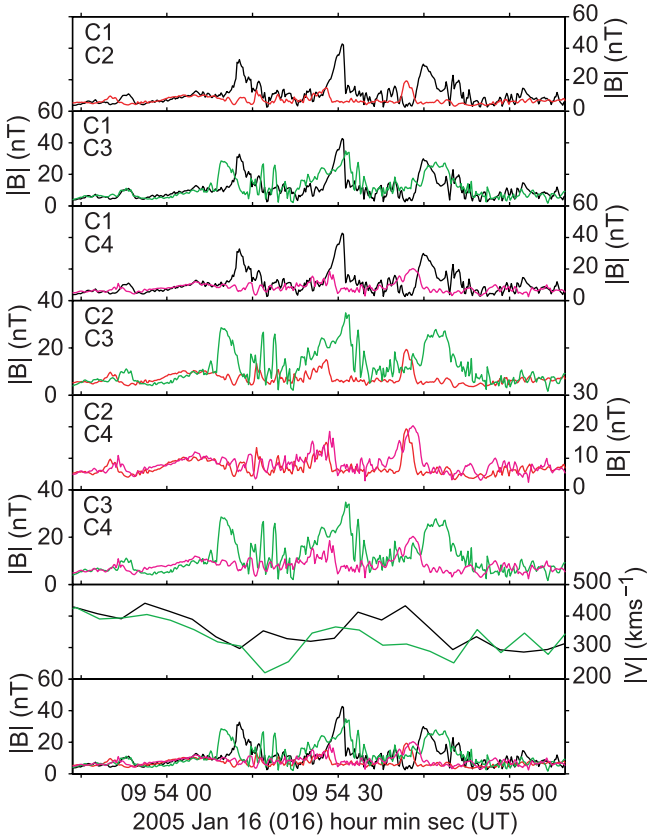

Figure 6. Comparison of the SLAMS magnetic field magnitude, |B|, between pairs of spacecraft. The same colors and line styles are used for all panels: Cluster 1: black; Cluster 2: red; Cluster 3: green; Cluster 4: magenta. The first through sixth panels show |B| from C1 and C2, C1 and C3, C1 and C4, C2 and C3, and C2 and C4, respectively. For reference, the seventh panel shows the velocity magnitude |V| from C1 and C3, and the eighth panel replots the magnetic field magnitude from all four spacecraft.

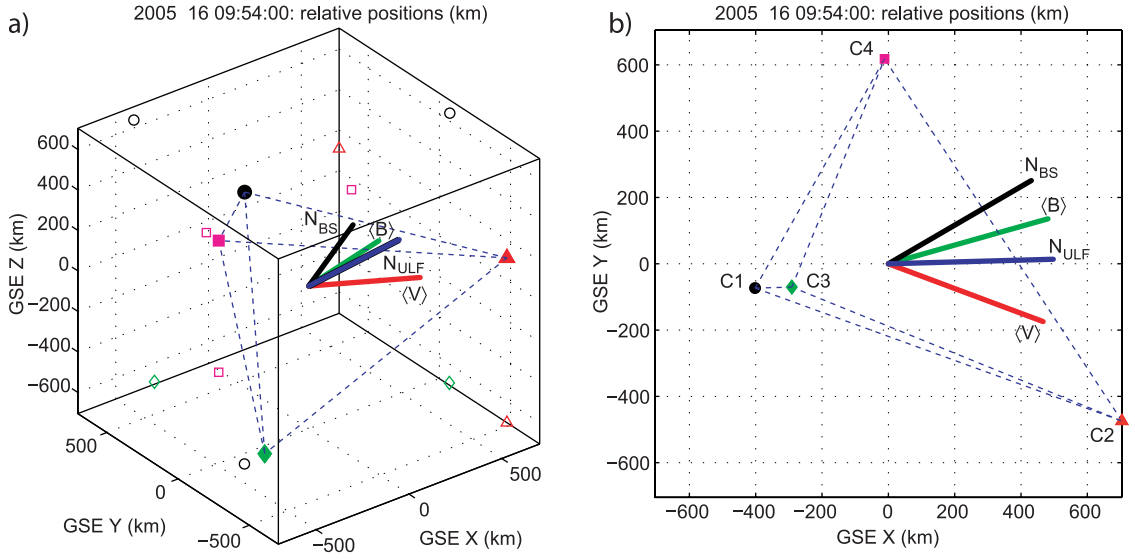

Figure 7. (a) Cluster tetrahedron configuration at 0954 UT on 16 January 2005. Spacecraft positions are shown relative to the center of the formation in km, in GSE coordinates. Filled symbols represent the spacecraft positions: C1: black circle, C2: red triangle, C3: green diamond, and C4: magenta square. Open symbols indicate the projection of the spacecraft positions onto the three sides of the box. Labeled vectors indicate the following directions, plotted with a positive X_{GSE} component: model bow shock normal (N_{BS}), average magnetic field direction ($\langle B \rangle$), average normal direction for upstream ULF waves (N_{ULF}) and average plasma flow vector ($\langle V \rangle$). (b) The same figure projected onto the X-Y_{GSE} plane.

magnetic field magnitude signatures between each of the six pairs of spacecraft. The seventh panel shows the plasma velocity from Cluster 1 and Cluster 3, while the bottom panel shows the magnetic field magnitude from all four spacecraft.

[27] Figure 7 shows the tetrahedron configuration during this shock transition and illustrates why this is a useful case study. Figure 7a shows a three-dimensional representation of the tetrahedron plotted relative to the center of the formation: C1 (filled circle), C2 (filled triangle), C3 (filled diamond), and C4 (filled square). Also shown in the open symbols are the spacecraft positions projected onto each face of the cube. Vectors are shown centered at the middle of the formation to indicate the average plasma flow vector during the interval, $\langle V \rangle$, the model bow shock normal, N_{BS}, and the average magnetic field direction, $\langle B \rangle$. Also shown for comparison with the spacecraft separation vector is the average ULF wave normal direction, N_{ULF} = [0.995, 0.027, 0.097], calculated using spacecraft timing for the interval of ULF wave activity observed following the shock encounter (0956:00–0959:45 UT). From this figure it can be seen that C1, C2, and C4 lie in a plane nearly parallel to the X-Y_{GSE} plane and that Cluster 3 lies below Cluster 1 in Z_{GSE}. At this time Cluster was located at [9.9, 13.2, 2.1] R_E (GSE): close to the X-Y_{GSE} plane. Therefore the model bow shock normal and the solar wind flow vector are also largely confined to the X-Y_{GSE} plane. Thus, Figure 7b shows the tetrahedron at the same time, but projected onto the X-Y_{GSE} plane which makes it easier to compare the different spacecraft separation vectors with the bow shock normal and plasma flow velocity directions. The velocity vector is deflected from the radial direction since during this period the plasma is partially shocked.

[28] The normal calculated for the upstream ULF waves N_{ULF} lies within 5° of the radial direction, and the order in which the waves are convected across the Cluster tetrahedron (not shown) is C2 then C4, followed by C1 and C3 nearly simultaneously. Figure 7 shows that C2 and C4 are separated in a direction approximately perpendicular to the model bow shock normal, N_{BS}, and thus lie close to parallel to the expected shock plane. Therefore if SLAMS become refracted to have an orientation approximately parallel to the expected shock surface, they should be seen almost simultaneously at C2 and C4, despite the two satellites having a significant separation parallel to the flow velocity vector, in contrast to the behavior of the ULF waves. Since C1 and C3 are separated predominately in Z_{GSE} any structure with a normal largely confined to the X-Y_{GSE} plane will cross those two spacecraft nearly simultaneously. However, C1 and C3 both lie earthward of C2 and C4 relative to the expected bow shock orientation. Thus we might expect SLAMS to be of greater amplitude at C1 and C3 and to be seen at both spacecraft at the same time.

[29] Figure 6 shows comparisons between the six pairs of spacecraft. The fifth panel shows Cluster 2 and C4, which are separated in a direction approximately parallel to the bow shock surface. The pulsations in the fifth panel are seen nearly simultaneously, consistent with their refraction to become parallel to the shock surface, with a substantially smaller delay between the two spacecraft than would be expected if the pulsations retained the orientation of the upstream ULF waves. The second panel shows data from C1 and C3. As expected the pulsations are also seen nearly simultaneously at this pair of spacecraft, although the correlation between the signatures is less good, perhaps reflecting the larger separation of the spacecraft in Z_{GSE}.

However, the amplitude of the pulsations is greater, consistent with their rapid growth as they are convected toward the shock. This can also be seen in panel 1 showing data from C2 and C1. C2 was situated further upstream of C1 and observed smaller-amplitude SLAMS. The SLAMS at C2 and C4 (fifth panel) are the same amplitude, suggesting that this is indeed growth rather than a spatial gradient in pulsation size.

[30] Finally, the sixth panel shows data from C4 and C3. These two spacecraft have only a 350 km separation along N_{ULF} yet the delay between the SLAMS at the two spacecraft is ~4.5 s: several times longer than would be expected if the SLAMS retained the ULF wave direction, even taking into account the slowed and deflected plasma flow vector.

[31] These results are consistent with SLAMS being refracted very close to where the shock thermalization is occurring, perhaps associated with the SLAMS contributing to those processes through their interaction with the plasma. The simultaneous observation of the same structures at Cluster 2 and Cluster 4, separated by ~1300 km parallel to the shock surface, supports the suggestion that the SLAMS have an overall size exceeding a thousand kilometers in this direction and also demonstrates that they have a coherence length greater than this distance parallel to the shock surface. That several structures are seen simultaneously at these two spacecraft also suggests that there is a consistent underlying orientation of SLAMS over this distance and that that the variety of orientations shown in Figure 4b is likely to be a signature of local ripples in the SLAM structures.

[32] The conclusions that we can draw from a single case study are limited. During this day when Cluster crossed and recrossed the shock there are a number of times at which similar (though less clear) signatures occur (e.g., ~0918, 0933, 0936, and 0944 UT). They all occur during periods when the plasma is partially shocked, but not every velocity transition exhibits such behavior. Ideally, we would identify intervals consistent with SLAMS refraction using objective selection criteria in order to quantify when and under what conditions this effect occurs and to test whether the change in SLAMS orientation is always ordered by the model shock normal. However, the correlation between the signatures at the different spacecraft is significantly lower within the shock than during intervals of upstream ULF wave activity, even for pairs of spacecraft that observe the SLAMS at nearly the same time. The correlation between spacecraft is also sometimes low in the magnetosheath immediately downstream of the shock, and therefore, so far, it has not been possible to make this kind of systematic analysis. Thus, on the basis of this shock we conclude that some regions of partially shocked plasma contain SLAMS with signatures consistent with them having been refracted to lie parallel to the shock surface, although we cannot yet confirm that SLAMS refraction is a fundamental feature of the quasi-parallel shock.

3. Discussion and Conclusions

[33] In this paper we have considered several aspects of the quasi-parallel bow shock and properties of SLAMS embedded within the transition not previously studied using observational data: SLAMS growth, the thickness of the shock transition, and whether SLAMS are refracted as they are convected toward the shock. In addition we were able to use the four-point Cluster data to give further insight into the size and shape of SLAMS on scales of thousands of kilometers. This complemented earlier work which showed that SLAMS contained variations in their magnetic field signatures on scales as small as a few hundred km, despite their overall size exceeding ~1000 km, in contrast with the much longer correlation lengths associated with upstream ULF waves.

[34] New Cluster observations confirm that SLAMS exhibit rapid growth. Comparing SLAMS observations at 100, 250, and 1000 km shows that unless the time delay between observations of the pulsations at different spacecraft is less than a second or so, the effect of SLAMS growth cannot be neglected. Ideally, we would extend this study by preconditioning the data in order to reduce the influence of spatial variations on these results, for example by preferentially selecting observations where a pair of spacecraft had a small separation perpendicular to the flow. However, it was found that the flow perpendicular and flow parallel separations were correlated, and with the current observations it was not possible to divide the data set into two independent subsets.

[35] Evidence for the overall thickness of the quasi-parallel shock being rather narrow came from a crossing observed by Cluster on 22 February 2005 when the spacecraft were in a formation with a scale ~1000 × 3000 km. For a period of over 10 min one spacecraft was clearly located upstream in the foreshock while another remained in the magnetosheath, despite the interspacecraft separation being only 2700 km along the estimated model shock normal. In addition, for several shorter periods of about a minute in between multiple shock crossings, a pair of spacecraft separated by ~1200 km straddled the shock transition. Therefore, for this crossing we conclude that the thickness of the region in which the bulk of the plasma thermalization occurred was in general less than 2700 km and for at least some times less than 1200 km. This suggests that at most a few, but probably sometimes only a single SLAM structure contributes to plasma thermalization at any one time. The multiple shock encounters made by the more closely separated spacecraft might arise from large-scale shock motion, but it could also indicate a variation in the thickness of the shock, consistent with the process of shock reformation.

[36] In order to test whether SLAMS undergo a systematic change in orientation as they grow from ULF waves, it is necessary to compare SLAMS signatures at the four spacecraft. In a first attempt to reduce the influence of SLAMS growth, a set of SLAMS sampled with the smallest tetrahedron scale of 100 km was analyzed to calculate their orientations. We looked for a systematic change in orientation, using the suprathermal ion number density (ions with energy > 1.2 keV) as a first-order proxy for distance from the shock. Although the size of the SLAMS was well ordered by this parameter, the SLAMS orientations were not, and they exhibited a wide scatter that was greater than that found for a set of ULF waves during the same orbit. On the basis of these results alone, the variation in SLAMS directions could be explained by (1) SLAMS not having an

underlying orientation or (2) SLAMS being rippled on these small scales.

[37] In order to explore which of these two was more likely we used a shock crossing on 16 January 2005 at which a fortuitous tetrahedron orientation relative to the nominal shock surface allowed us to study SLAMS orientations on ~1000 km scales without increasing the influence of SLAMS growth. During this orbit the tetrahedron configuration was such that pairs of spacecraft were separated in directions perpendicular to the plasma flow vector, parallel to the model shock normal, and, most importantly, parallel to the expected underlying shock surface. This formation gave us a better chance of observing SLAMS nearly simultaneously at two widely separated spacecraft, should the SLAMS be lying parallel to the shock surface, thus reducing the influence of SLAMS growth on the signature. Having earlier analyzed a shock at which we were able to place an upper limit of only a few thousand kilometers on the region where the shock had the bulk of its effect led us to concentrate on regions where a substantial change in velocity was observed, in order to look for evidence of SLAMS refraction close to the shock.

[38] A variety of signatures were observed in regions where the plasma flow velocity was changing, perhaps reflecting the varying contributions of spatial variation and time evolution of the shock layer as it passed over the spacecraft. However, at several transitions, signatures consistent with SLAMS refraction were observed. The simultaneous observation of SLAMS at two spacecraft separated along the shock surface not only showed that SLAMS are coherent over a distance of ~1300 km transverse to the shock normal but also suggested that there is a consistent underlying orientation of SLAMS over this distance, at least close to the shock. We would like to extend this study to include other shock crossings, in order to establish whether or not SLAMS refraction is a fundamental feature of the quasi-parallel shock, but so far further cases with such a favorable tetrahedron configuration have not yet been identified.

[39] The results from this study suggest that the variety of SLAMS orientations found using data at 100 km scales cannot be explained by the lack of an underlying SLAMS orientation, at least for those events associated with higher suprathermal number densities close to the shock. It is possible that we had too few of these events to allow the signature of refraction to be observed or that the suprathermal number density was not a sufficiently sensitive measure of distance from the shock for it to order the observations. However, we suggest that it is possible that the variety of SLAMS orientations found even for those events far from the shock, in comparison with the range of orientations found for ULF waves, might be indicative of the presence of small-scale ripples and we plan to address this question further using data recorded with tetrahedron scales larger than 100 km.

[40] These results can be combined to give an overall picture of the quasi-parallel shock as a basis for further analysis. This picture is similar to the schematic proposed by *Schwartz and Burgess* [1991], although we now have evidence for smaller scale variability and perhaps a narrower region where most of the plasma thermalization occurs. SLAMS grow from the upstream ULF waves as they are convected antisunward into the energetic particle pressure gradient. *Archer et al.* [2005] showed that the ULF wave correlation length perpendicular to their wave vector direction was of the order of the scale of the bow shock itself. Thus, we would expect an underlying large-scale orientation to be retained by the SLAMS, even though smaller-scale variations, at hundreds to thousands of kilometers, are also observed. Although the foreshock is quite extended, these results suggest that at any one time the main shock transition is narrow, of the order of one or a few thousand kilometers, consisting of a single or perhaps a few pulsations which refract as they approach this region to lie parallel to the nominal shock surface, and that the shock transition is continually reforming as new SLAMS grow rapidly to replace those that pass downstream.

[41] **Acknowledgments.** Cluster research at Imperial College London is supported by STFC. EAL is supported by a PPARC (now STFC) Advanced Fellowship.

[42] Amitava Bhattacharjee thanks Jonathan Eastwood and another reviewer for their assistance in evaluating this paper.

References

Archer, M., T. S. Horbury, E. A. Lucek, C. Mazelle, A. Balogh, and I. Dandouras (2005), Size and shape of ULF waves in the terrestrial foreshock, *J. Geophys. Res.*, *110*, A05208, doi:10.1029/2004JA010791.

Bale, S. D., et al. (2005), Quasi-perpendicular shock structure and processes, *Space Sci. Rev.*, *118*, 161–203, doi:10.1007/s11214-005-3827-0.

Balogh, A., et al. (2001), The Cluster magnetic field investigation: overview of in-flight performance and initial results, *Ann. Geophys.*, *19*, 1207–1217.

Burgess, D. (1989), Cyclic behaviour at quasi-parallel collisionless shocks, *Geophys. Res. Lett.*, *16*, 345–348, doi:10.1029/GL016i005p00345.

Burgess, D. (1995), Foreshock-shock interaction at collisionless quasi-parallel shocks, *Adv. Space Res.*, *15*(8/9), 159–169, doi:10.1016/0273-1177(94)00098-L.

Burgess, D., et al. (2005), Quasi-parallel shock structure and processes, *Space Sci. Rev.*, *118*(1–4), 205–222, doi:10.1007/s11214-005-3832-3.

Dubouloz, N., and M. Scholer (1995), Two-dimensional simulations of magnetic pulsations upstream of the Earth's bow shock, *J. Geophys. Res.*, *100*, 9461–9474, doi:10.1029/94JA03239.

Farris, M. H., C. T. Russell, and M. F. Thomsen (1993), Magnetic structure of the low beta, quasi-perpendicular shock, *J. Geophys. Res.*, *98*, 15,285–15,294, doi:10.1029/93JA00958.

Giacalone, J., S. J. Schwartz, and D. Burgess (1993), Observations of suprathermal ions in association with SLAMS, *Geophys. Res. Lett.*, *20*, 149–152, doi:10.1029/93GL00067.

Giacalone, J., S. J. Schwartz, and D. Burgess (1994), Artificial spacecraft in hybrid simulations of the quasi-parallel Earth's bow shock: Analysis of time series versus spatial profiles and a separation strategy for Cluster, *Ann. Geophys.*, *12*, 591–601, doi:10.1007/s00585-994-0591-5.

Gosling, J. T., M. F. Thomsen, S. J. Bame, W. C. Feldman, G. Paschmann, and N. Sckopke (1982), Evidence for specularly reflected ions upstream of from the quasi-parallel bow shock, *Geophys. Res. Lett.*, *9*, 1333–1336, doi:10.1029/GL009i012p01333.

Gosling, J. T., M. F. Thomsen, and S. J. Bame (1989), Ion reflection and downstream thermalisation at the quasi-parallel bow shock, *J. Geophys. Res.*, *94*, 10,027–10,037, doi:10.1029/JA094iA08p10027.

Greenstadt, E. W., M. M. Hoppe, and C. T. Russell (1982), Large-amplitude magnetic variations in quasi-parallel shocks: Correlation lengths measured by ISEE 1 and 2, *Geophys. Res. Lett.*, *9*, 781–784, doi:10.1029/GL009i007p00781.

Horbury, T. S., P. J. Cargill, E. A. Lucek, J. Eastwood, A. Balogh, M. W. Dunlop, K.-H. Fornaçon, and E. Georgescu (2002), Four spacecraft measurements of the quasi-perpendicular terrestrial bowshock: Orientation and motion, *J. Geophys. Res.*, *107*(A8), 1208, doi:10.1029/2001JA000273.

Ipavich, F. M., A. Galvin, G. Gloeckler, M. Scholer, and D. Hovestadt (1981), A statistical survey of ions observed upstream of the earth's bow shock – Energy spectra, composition, and spatial variation, *J. Geophys. Res.*, *86*, 4337–4342, doi:10.1029/JA086iA06p04337.

Kis, A., M. Scholer, B. Klecker, E. Möbius, E. Lucek, H. Rème, J. M. Bosqued, L. M. Kistler, and H. Kucharek (2004), Multispacecraft observations of diffuse ions upstream of the Earth's bow shock, *Geophys. Res. Lett.*, *31*, L20801, doi:10.1029/2004GL020759.

Le, G., and C. T. Russell (1990), A study of the coherence length of ULF waves in the Earth's foreshock, *J. Geophys. Res.*, *95*, 10,703–10,706, doi:10.1029/JA095iA07p10703.

Le, G., and C. T. Russell (1992), A study of ULF wave foreshock morphology? II: Spatial variation of ULF waves, *Planet. Space Sci.*, *40*, 1215–1225, doi:10.1016/0032-0633(92)90078-3.

Lucek, E. A. (2006), SLAMS at parallel shocks and hot flow anomalies, in *Proceedings of Cluster and Double Star Symposium – 5th Anniversary of Cluster in Space*, edited by K. Fletcher, *Eur. Space Agency Spec. Publ.*, *ESA SP 598*.

Lucek, E. A., T. S. Horbury, M. W. Dunlop, P. J. Cargill, S. J. Schwartz, A. Balogh, P. Brown, C. Carr, K.-H. Fornaçon, and E. Georgescu (2002), Cluster magnetic field observations at a quasi-parallel bow shock, *Ann. Geophys.*, *20*, 1699–1710.

Lucek, E. A., T. S. Horbury, A. Balogh, I. Dandouras, and H. Rème (2004), Cluster observations of structure at quasi-parallel bow shocks, *Ann. Geophys.*, *22*, 1–5.

Mann, G., H. Lühr, and W. Baumjohann (1994), Statistical analysis of short large-amplitude magnetic field structures in the vicinity of the quasi-parallel bow shock, *J. Geophys. Res.*, *99*, 13,315–13,323, doi:10.1029/94JA00440.

Onsager, T. G., M. F. Thomsen, J. T. Gosling, S. J. Bame, and C. T. Russell (1990), Survey of coherent ion reflection at the quasi-parallel bow shock, *J. Geophys. Res.*, *95*, 2261–2274, doi:10.1029/JA095iA03p02261.

Paschmann, G., N. Sckopke, S. J. Bame, and J. T. Gosling (1982), Observations of gyrating ions in the foot of the nearly-perpendicular bow shock, *J. Geophys. Res.*, *93*, 881–884.

Peredo, M., J. A. Slavin, E. Mazur, and S. A. Curtis (1995), Three-dimensional position and shape of the bow shock and their variation with Alfvénic, sonic and magnetosonic Mach numbers and interplanetary field orientation, *J. Geophys. Res.*, *100*, 7907–7916, doi:10.1029/94JA02545.

Rème, H., et al. (2001), First multispacecraft ion measurements in and near the Earth's magnetosphere with the identical Cluster ion spectrometry (CIS) experiment, *Ann. Geophys.*, *19*, 1303–1354.

Scholer, M. (1993), Upstream waves, shocklets, short large-amplitude magnetic structures and the cyclic behavior of oblique quasi-parallel collisionless shocks, *J. Geophys. Res.*, *98*, 47–57, doi:10.1029/92JA01875.

Scholer, M., H. Kucharek, and I. Shinohara (2003), Short large-amplitude magnetic structures and whistler wave precursors in a full-particle quasi-parallel shock simulation, *J. Geophys. Res.*, *108*(A7), 1273, doi:10.1029/2002JA009820.

Schwartz, S. J. (1998), Shock and discontinuity normals, Mach number and related parameters, in *Analysis Methods for Multi-Spacecraft Data*, edited by G. Paschmann and P. W. Daly, pp. 249–270, ESA Publ. Div., Noordwijk, Netherlands.

Schwartz, S. J., and D. Burgess (1991), Quasi-parallel shocks: A patchwork of three-dimensional structures, *Geophys. Res. Lett.*, *18*, 373–376, doi:10.1029/91GL00138.

Schwartz, S. J., D. Burgess, W. P. Wilkinson, R. L. Kessel, M. Dunlop, and H. Lühr (1992), Observations of short large-amplitude magnetic structures at a quasi-parallel shock, *J. Geophys. Res.*, *97*, 4209–4227, doi:10.1029/91JA02581.

Sckopke, N., G. Paschmann, A. L. Brinca, C. W. Carlson, and H. Lühr (1990), Ion thermalisation in quasi-perpendicular shocks involving reflected ions, *J. Geophys. Res.*, *95*, 6337–6352, doi:10.1029/JA095iA05p06337.

Thomsen, M. F., J. T. Gosling, and C. T. Russell (1988), ISEE studies of the quasi-parallel bow shock, *Adv. Space Res.*, *8*, 9175–9178.

Thomsen, M. F., J. T. Gosling, T. G. Onsager, and C. T. Russell (1993), Ion and electron heating at the low-mach-number quasi-parallel bow shock, *J. Geophys. Res.*, *98*, 3875–3888, doi:10.1029/92JA02560.

Trattner, K. J., E. Möbius, M. Scholer, B. Klecker, M. Hilchenbach, and H. Lühr (1994), Statistical analysis of diffuse ion events upstream of the Earth's bow shock, *J. Geophys. Res.*, *99*, 13,389–13,400.

Tsubouchi, K., and B. Lembège (2004), Full particle simulations of short large-amplitude magnetic structures (SLAMS) in quasi-parallel shocks, *J. Geophys. Res.*, *109*, A02114, doi:10.1029/2003JA010014.

Tsurutani, B. T., and R. G. Stone (Eds.) (1985), *Collisionless Shocks in the Heliosphere: Reviews of Current Research*, *Geophys. Monogr. Ser.*, vol. 35, AGU, Washington, D. C.

I. Dandouras and H. Rème, Centre d'Etude Spatiale des Rayonnements, 9 Avenue du Colonel Roche B.P. 4346, Toulouse, F-31028 France.

T. S. Horbury and E. A. Lucek, Blackett Laboratory, Imperial College London, London SW7 2AZ, UK. (e.lucek@imperial.ac.uk)